

## FACTORS AFFECTING LATERAL STABILITY

By John P. Campbell

Langley Aeronautical Laboratory

## INTRODUCTION

The term "lateral stability" used in this paper is intended to include all airplane stability other than longitudinal stability. That is, lateral stability includes directional (or weathercock) stability, rolling stability, bank stability (or dihedral effect) and, in fact, any form of stability that involves displacement of the plane of symmetry of the airplane by rolling, yawing, or sideslipping. Sometimes the term "lateral stability" has been used to mean only the stability associated with rolling moment due to sideslip or dihedral effect but this usage is not recommended because of the likelihood of confusion with the more general meaning of the term.

During the past few years many advances have been made toward an understanding of the complex problem of lateral stability. In the war years a great amount of experimental data on the subject was obtained from studies of military airplane designs. Analysis and correlation of these data have afforded an insight into the causes of lateral-stability difficulties and have in some cases permitted empirical methods to be set up for estimating certain stability characteristics. Basic lateral-stability research, both experimental and theoretical, was necessarily somewhat curtailed during the war but since that time this research has been accelerated to supply the ever-increasing demand for fundamental knowledge in the field of lateral stability.

## SYMBOLS

|        |                                    |   |
|--------|------------------------------------|---|
| $C_L$  | lift coefficient                   | $\left( \frac{\text{Lift}}{\frac{1}{2}\rho V^2 S} \right)$  |
| $C_l$  | rolling-moment coefficient         | $\left( \frac{\text{Rolling moment}}{\frac{1}{2}\rho V^2 S b} \right)$                                    |
| $C_n$  | yawing-moment coefficient          | $\left( \frac{\text{Yawing moment}}{\frac{1}{2}\rho V^2 S b} \right)$                                     |
| $C_n'$ | fuselage yawing-moment coefficient | $\left( \frac{\text{Yawing moment}}{\left( \frac{1}{2}\rho V^2 \right) (\text{Fuselage volume})} \right)$ |

|                 |  |
|-----------------|--|
| $C_Y$           | lateral-force coefficient $\left( \frac{\text{Lateral force}}{\frac{1}{2}\rho V^2 S} \right)$  |
| $C_{D_w}$       | wing-drag coefficient $\left( \frac{\text{Drag}}{\frac{1}{2}\rho V^2 S} \right)$   |
| $\rho$          | mass density, slugs per cubic foot   |
| $S$             | wing area, square feet   |
| $b$             | wing span, feet  |
| $z$             | vertical height of wing above fuselage center line, feet   |
| $V$             | airspeed, feet per second  |
| $v$             | sideslip velocity, feet per second   |
| $\beta$         | angle of sideslip  |
| $\psi$          | angle of yaw ( $\beta = -\psi$ )   |
| $\alpha$        | angle of attack  |
| $p$             | rolling angular velocity, radians per second   |
| $r$             | yawing angular velocity, radians per second  |
| $\frac{pb}{2V}$ | rolling-angular-velocity factor or wing-tip helix angle generated by wing tip in roll, radians                                       |
| $\frac{rb}{2V}$ | yawing-angular-velocity factor, radians  |
| $C_{n\beta}$    | rate of change of yawing-moment coefficient with angle of sideslip, per degree $\left( \frac{\partial C_n}{\partial \beta} \right)$  |
| $C_{l\beta}$    | rate of change of rolling-moment coefficient with angle of sideslip, per degree $\left( \frac{\partial C_l}{\partial \beta} \right)$ |
| $C_{Y\beta}$    | rate of change of lateral-force coefficient with angle of sideslip, per degree $\left( \frac{\partial C_Y}{\partial \beta} \right)$  |

|            |  |
|------------|--|
| $C_{n_p}$  | rate of change of yawing-moment coefficient with rolling-angular-velocity factor, per radian $\left(\frac{\partial C_n}{\partial \frac{pb}{2V}}\right)$  |
| $C_{l_p}$  | rate of change of rolling-moment coefficient with rolling-angular-velocity factor, per radian $\left(\frac{\partial C_l}{\partial \frac{pb}{2V}}\right)$ |
| $C_{Y_p}$  | rate of change of lateral-force coefficient with rolling-angular-velocity factor, per radian $\left(\frac{\partial C_Y}{\partial \frac{pb}{2V}}\right)$  |
| $C_{n_r}$  | rate of change of yawing-moment coefficient with yawing-angular-velocity factor, per radian $\left(\frac{\partial C_n}{\partial \frac{rb}{2V}}\right)$   |
| $C_{l_r}$  | rate of change of rolling-moment coefficient with yawing-angular-velocity factor, per radian $\left(\frac{\partial C_l}{\partial \frac{rb}{2V}}\right)$  |
| $C_{Y_r}$  | rate of change of lateral-force coefficient with yawing-angular-velocity factor, per radian $\left(\frac{\partial C_Y}{\partial \frac{rb}{2V}}\right)$   |
| $\delta_f$ | flap deflection, degrees   |
| $\Lambda$  | angle of sweep of wing leading edge, degrees   |
| A          | aspect ratio $\left(\frac{b^2}{S}\right)$  |

#### LATERAL-STABILITY DERIVATIVES

In a discussion of lateral stability it is necessary to break up this rather complex subject into its several related parts in order to get a clear picture of the advances that have recently been made in this field. One logical breakdown of lateral stability, illustrated in figure 1, involves the conventional lateral-stability derivatives used in dynamic lateral-stability work. (See references 1 to 6.) These stability derivatives are abbreviated expressions for the variations of

the rolling and yawing moments and lateral force with sideslipping, rolling, and yawing velocities. In order to make these derivatives nondimensional, the velocities  $v$ ,  $p$ , and  $r$  are replaced by  $\beta$  (or  $\frac{v}{V}$ ),  $\frac{pb}{2V}$ , and  $\frac{rb}{2V}$ , respectively, as indicated at the bottom of figure 1. (See reference 1.)

The geometric designs around the derivatives in figure 1 indicate their relative importance as determined from an analysis of many theoretical and experimental studies of lateral stability. The circled derivatives have been found to be most important in that, if they are properly adjusted, the other derivatives usually have only minor effects on stability. In a discussion of lateral stability, these derivatives may logically be divided into three groups - sideslip, rolling, and yawing derivatives.

#### Sideslip Derivatives

The sideslip derivatives  $C_{n\beta}$ ,  $C_{l\beta}$ , and  $C_{Y\beta}$  are probably the most significant as well as the most familiar derivatives. They can be determined theoretically (references 1, 2, 6, and 7) and are also easily determined by ordinary wind-tunnel tests (references 8 to 19) in which the lateral forces and moments are measured with the model in a yawed (or sideslipped) attitude. From plots of the force-test data, the slopes  $\frac{\partial C_n}{\partial \psi}$ ,  $\frac{\partial C_l}{\partial \psi}$ , and  $\frac{\partial C_Y}{\partial \psi}$  (where  $\psi$  is the angle of yaw) are determined and these values are exactly equal to but opposite in sign to  $C_{n\beta}$ ,  $C_{l\beta}$ , and  $C_{Y\beta}$ , respectively. The yawing moment due to sideslip  $C_{n\beta}$  is the static directional stability or weathercock-stability factor (references 20 to 34). The rolling moment due to sideslip  $C_{l\beta}$  is the well-known effective-dihedral parameter which has received an increasing amount of attention in connection with highly swept wings. (See references 5, 19, 35, 36, and 37.) The lateral force due to sideslip  $C_{Y\beta}$  is the effective lateral-area parameter, which is usually negligible if the weathercock stability  $C_{n\beta}$  is adequate. This derivative will not be discussed further in this paper but more information on it can be obtained in references 1, 2, 6, and 38.

#### Rolling Derivatives

The rolling derivatives  $C_{n_p}$ ,  $C_{l_p}$ , and  $C_{Y_p}$  have been treated theoretically in references 2, 6, and 39 and are measured by various experimental methods including continuous rotation tests (reference 40)

in which forces and moments are measured on a rolling model and rolling-flow tests in which the model remains stationary while the air stream in the wind tunnel is rotated (Langley stability tunnel, reference 41). Both the yawing moment due to rolling  $C_{n_p}$  and the rolling moment due to rolling (damping-in-roll factor)  $C_{l_p}$  are important from considerations of controllability as well as stability. The lateral force due to rolling  $C_{y_p}$  is of measurable magnitude only for swept-wing airplanes and, since in all cases this derivative has been found to have an insignificant effect on stability, it will not be discussed further.

### Yawing Derivatives

The yawing derivatives  $C_{n_r}$ ,  $C_{l_r}$ , and  $C_{y_r}$  are of secondary importance compared with the sideslip and rolling derivatives. These derivatives are treated theoretically in references 1, 6, 42, and 43 and have been determined experimentally by several methods including the whirling-arm method, forced-oscillation or free-oscillation method (reference 44), and the curved-flow method (Langley stability tunnel, reference 6), in which a model is held fixed in a curving air stream produced by curving the flexible side walls of the tunnel test section. The yawing moment due to yawing (damping-in-yaw parameter)  $C_{n_r}$  is the most important of the yawing derivatives but usually has no pronounced effects on stability and control if the weathercock stability  $C_{n_\beta}$  is adequate. Since the rolling moment due to yawing  $C_{l_r}$  and the lateral force due to yawing  $C_{y_r}$  are even less important than  $C_{n_r}$ , no further discussion of the yawing derivatives will be given. More information on these derivatives can be found in the references 1, 6, 43, and 44.

### MOST IMPORTANT LATERAL-STABILITY DERIVATIVES

The four most important derivatives  $C_{n_\beta}$ ,  $C_{l_\beta}$ ,  $C_{n_p}$ , and  $C_{l_p}$  will now be considered in more detail. The main emphasis will be placed on the two sideslip derivatives  $C_{n_\beta}$  and  $C_{l_\beta}$  since these derivatives have been the subject of a large part of the lateral-stability research during the past few years.

#### Yawing Moment Due to Sideslip $C_{n_\beta}$

The yawing moment due to sideslip  $C_{n_\beta}$  is a direct indication of the tendency of an airplane to weathercock, that is, to keep aligned with

the relative wind. Since the wing-fuselage combination is usually unstable in this respect, a vertical tail is used which is large enough to balance out this instability and to provide a satisfactory amount of weathercock stability. This concept is very simple, but in practice proportioning an airplane to obtain a desired amount of weathercock stability has proved to be quite difficult because so many factors affect this stability. The effects of some of the more important factors will now be treated briefly.

Effect of vertical-tail aspect ratio.- One rather obvious point, but one which has not been fully appreciated until recent years, is the effect of the aspect ratio of the vertical tail on weathercock stability. This effect is illustrated in figure 2. Most airplanes prior to World War II had low-aspect-ratio vertical tails like that shown in solid lines on the sketch. The desire to get increased stability without an increase in tail area on many of our military airplanes led to use of vertical tails of higher aspect ratio which, because of their higher lift-curve slopes, gave more weathercock stability. This effect is clearly shown in figure 2 by a comparison of the slopes of yawing-moment curves  $\left(\frac{\partial C_n}{\partial V} \text{ or } C_{n\beta}\right)$  for a model tested with two tails of equal area but of aspect ratios of 1.0 and 2.3.

End-plate effect of horizontal tail.- Another factor which has to be taken into account in estimating vertical-tail effectiveness is the end-plate effect of the horizontal tail. Recent NACA research on this subject (references 29 and 31) has helped to put the estimation of this effect on a rational basis. In figure 3 a part of this research is summarized to show how the vertical-tail effectiveness is increased by the end-plate effect when the horizontal tail is located near the bottom or top of the vertical tail. In general, the effects of the fore and aft position of the horizontal tail and the relative sizes of the horizontal and vertical tails are small when compared with the effect of the vertical position of the horizontal tail.

Effect of wing position.- The effect of the vertical position of the wing on the fuselage on weathercock stability is illustrated in figure 4, which is a plot of the increment in  $C_{n\beta}$  produced by changing from a midwing configuration to a high- or low-wing configuration. It is apparent from these data that a pronounced decrease in stability occurs as the wing is moved from a low to a high position. The amount of this reduction in  $C_{n\beta}$  (over 0.001) is more than one-half the increment in  $C_{n\beta}$  provided by a vertical tail of average size. This effect of wing position results primarily from the difference in the sidewash induced at the vertical tail by the high-wing and low-wing configurations. More information on this effect is given in references 9 to 13 and reference 30. Some of these references also cover the effects on  $C_{n\beta}$  of flaps, wing plan form, fuselage shape, and other factors.

Effect of power.— The effect of power on the weathercock stability of propeller-driven airplanes (references 32 to 34 and 45 to 53) has been the subject of extensive study in the last few years because the tremendous increase in the power of our military airplanes has greatly increased the difficulty of obtaining satisfactory stability under all operating conditions. In the case of multiengine airplanes one of the principal problems has been to design the airplane so that directional stability and trim characteristics are satisfactory with one or two engines on the same side inoperative. (See reference 33.)

In the case of high-powered single-engine airplanes there is an asymmetry in the power-on condition that is similar to the asymmetry caused on multiengine airplanes by the failure of one engine. This asymmetry is illustrated in figure 5 by the yawing-moment curve for the single-rotation power condition for a typical high-powered single-engine airplane. The effect of power is to increase the slope of the curve (indicating an increase in weathercock stability) and to displace the curve so that at zero yaw there is a large negative or left yawing moment. A  $20^\circ$  right rudder deflection was found necessary in this case to trim the airplane at zero yaw. With this single-rotation condition the propeller slipstream is displaced to the right at the vertical tail so that the tail passes out of the slipstream sooner when the airplane yaws to the right than when it yaws to the left. This effect causes the yawing-moment curve to break at about  $10^\circ$  for right yaw and about  $25^\circ$  for left yaw when the tail loses effectiveness as it passes out of the slipstream. The airplane tends to become directionally unstable when the tail passes out of the slipstream because the instability of the wing-fuselage-propeller combination is greatly increased by the application of power. This increased instability is caused partly by the lateral force on the propeller itself and partly by the slipstream effect on the wing-fuselage combination.

The undesirable asymmetry with power on is of course not present on jet-propelled airplanes, and it appears that power in this case has little, if any, effect on weathercock stability. Efforts at minimizing the asymmetry on propeller-driven airplanes have been attempted by several methods, such as offsetting the vertical tail, shifting the center of gravity to the right of the thrust axis (reference 54), skewing the thrust axis (reference 55), or using dual-rotating propellers (references 32 and 47). A comparison of dual and single rotation is shown in figure 5. It is apparent that dual rotation entirely eliminates the asymmetry but that the undesirable tendency toward instability at the higher angles of yaw is still present. Since this instability, when accompanied by rudder-force reversal, can lead to the dangerous "rudder-lock" condition (reference 28), methods have been sought to improve the weathercock stability at high yaw angles. In order to improve this condition, many high-powered airplanes have dorsal or ventral fins. The functioning of these fins is explained in figure 6.

Effect of dorsal and ventral fins.— Figure 6 shows the weathercock stability of a fuselage with and without dorsal and ventral fins. The solid-line curve shows the normal fuselage instability which decreases with increasing angle of yaw. The dashed-line curve shows that the fins do not greatly affect the stability at small angles of yaw but that they make the fuselage very stable at high angles of yaw where increased stability is needed when the vertical tail loses effectiveness. This stabilizing effect of the dorsal and ventral fins has been attributed to a "spoiling" of the flow over the after part of the fuselage but a further analysis based on the experimental data of reference 25 indicates that the effect can be partly accounted for by the increasing slope of the fin normal-force curve with increasing angle of yaw. Such an effect is characteristic of surfaces having extremely low aspect ratio. (See references 56 and 57.)

#### Rolling Moment Due to Sideslip

The rolling moment due to sideslip  $C_{l\beta}$  is known as the effective-dihedral derivative because the principal effect of varying the geometric dihedral angle of the wing is to change this derivative. (See references 35 and 36.) As pointed out in the introduction,  $C_{l\beta}$  is sometimes called "lateral stability" because it is the derivative which tends to return the airplane to a wing-level attitude when it banks and starts sideslipping. Interest in this derivative has recently been greatly increased because of its extreme variation with sweepback and aspect ratio, as illustrated in figure 7.

Effect of wing plan form on  $C_{l\beta}$ .— The effect of wing plan form on the variation of  $C_{l\beta}$  with lift coefficient  $C_L$  is shown in figure 7. The solid-line curves are from experimental data from reference 6 and the dashed-line curves are theoretical values obtained from the same reference. The value of  $-C_{l\beta}$  for unswept wings of normal aspect ratio 5.2 increases slightly with increasing lift coefficient and the theoretical variation is in good agreement with the experimental data. In the case of the sweptback wings, at low lift coefficients  $-C_{l\beta}$  increases rapidly with lift coefficient as indicated by theory but at some moderate lift coefficient  $-C_{l\beta}$  reaches a maximum value and then drops off as the maximum lift is approached. This "drop-off," which is not predicted by the theory, is attributed to a partial separation of flow over the wing which cannot be taken into account by any of the theoretical methods now being used. The lift coefficient at which the experimental results drop off and no longer agree with the theory is influenced by many factors such as wing plan form, airfoil section, Reynolds number, and wing roughness. The drop-off occurs earliest with the more highly swept wings and with wings



having airfoils with a sharp leading edge. Increasing the Reynolds number usually makes the experimental results agree with the theory up to a higher lift coefficient but if the wing surface is rough the drop-off occurs at a fairly low lift coefficient regardless of the Reynolds number. The use of high-lift devices such as flaps and slots usually increases the maximum value of  $C_{l\beta}$  for a given wing. (See reference 19.)

The data of figure 7 show that the use of sweepforward tends to reverse the variation of  $-C_{l\beta}$  with lift coefficient. For the particular wing shown, the effect of the sweepforward at low lift coefficients is to eliminate the variation of  $-C_{l\beta}$  with lift coefficient associated with the unswept wing.

Effect of wing position on  $C_{l\beta}$ .— The vertical position of the wing on the fuselage has a pronounced effect on the value of  $C_{l\beta}$  for a complete airplane. This effect has been treated theoretically in reference 7 and has been investigated experimentally in several NACA research studies (references 9 to 13). The results of some of this experimental work are summarized in figure 8 which is a plot of the increment in  $C_{l\beta}$  produced by changing from a midwing position to a high- or low-wing position. These data show that lowering the wing causes a large reduction in effective dihedral ( $-C_{l\beta}$ ) and that raising the wing causes a corresponding increase in effective dihedral. The scale at the right side of the plot indicates that changing from a low-wing to a high-wing position corresponds approximately to increasing the geometric dihedral angle of the wing by  $9^\circ$  or  $10^\circ$ . (A change of  $1^\circ$  in geometric dihedral angle corresponds to a change in  $C_{l\beta}$  of about 0.0002.) The data presented in figure 8 are for unswept wings but the same general trends would probably be obtained with swept wings.

Effect of power on  $C_{l\beta}$ .— For high-powered propeller-driven airplanes, the application of power usually causes a reduction in  $C_{l\beta}$  which is most pronounced in the flap-down condition. (See references 37, 47, and 51.) This effect is illustrated in figure 9 in which rolling-moment data are presented for a high-powered single-engine airplane with power off and with single- and dual-rotating propellers operating. In the power-off condition a large amount of effective dihedral is indicated by the steep slope of the rolling-moment curve. For the single-rotation condition the application of power causes a large reduction in effective dihedral and also causes a negative rolling moment at zero yaw. The reduction in effective dihedral is caused by the fact that in a yawed or sideslipped attitude a greater portion of the propeller slipstream passes over the trailing wing than over the

leading wing. Since the dynamic pressure in the slipstream is much greater than that outside the slipstream, the trailing wing then produces a greater increment of lift due to power than is produced by the leading wing. A rolling moment therefore results which tends to raise the trailing wing. This effect is called a negative dihedral effect because it is the same as that exhibited by a wing having negative geometric dihedral. The out-of-trim rolling moment at zero yaw is caused by the propeller torque which is, of course, to the left for right-hand propeller operation.

This out-of-trim rolling moment is not obtained with the dual-rotating propeller because the propeller torques balance out. There is, however, an even more pronounced reduction in effective dihedral than in the case of single rotation. This reduction in effective dihedral with power corresponds to putting about  $18^\circ$  negative dihedral in the wing of this airplane. It should be pointed out, however, that this extreme effect is shown for the flap-down, power-on condition (usually called the "wave-off" condition) and that much smaller effects are usually obtained in the flap-up conditions. One proposed method for reducing the effect of power on the effective dihedral is the use of a linked differential flap system. (See reference 37.) In the case of jet-propelled airplanes the effect of power on  $C_{L\beta}$  is probably negligible in all cases.

#### Yawing Moment Due to Rolling

The yawing moment due to rolling  $C_{n_p}$  has some effect on lateral stability but its most important effect is usually on lateral maneuverability. It is the derivative which, together with the aileron-yawing-moment factor  $C_{n_{\delta_a}}$ , largely determines the sideslipping tendencies in an aileron roll. For unswept wings this derivative is usually negative as shown in figure 10 which means that in a right roll it causes a left or adverse yawing moment which tends to yaw the airplane out of the turn.

The theoretical and experimental results in figure 10 which were taken from reference 6 show that the value of  $C_{n_p}$  increases with lift coefficient up to the stall which means that the adverse yawing tendency should be greatest at high lift coefficients.

For the sweptback wing (fig. 10), the theory indicates greater negative values of  $C_{n_p}$  than for the unswept wing. The experimental data, however, do not agree with the theory in this case. These data show even larger negative values of  $C_{n_p}$  at low lift coefficients than are indicated by theory, but at a moderate lift coefficient (about 0.5 in this case) the data show a sharp change which results in very large

positive or favorable values of  $C_{n_p}$  at the higher lift coefficients. As in the case of the abrupt drop-off in the value of  $C_{l_\beta}$  of the sweptback wings, this sharp change in  $C_{n_p}$  is attributed to a partial separation of flow over the wing which is not taken into account by this theory (reference 6). An approximate indication of the lift coefficient at which this change takes place, however, can be obtained

by means of the simple expression  $C_{n_p} = - \frac{C_L - 1.1 \frac{dC_{D_w}}{d\alpha}}{8}$  from reference 1.

### Rolling Moment Due to Rolling

The rolling moment due to rolling  $C_{l_p}$  is called the damping-in-roll derivative because it is the factor which is a measure of the resistance of an airplane to pure rolling motions. Considerable theoretical and experimental work (references 2, 6, 39, 40, 41, 57, 58, and 59) has been done on this derivative because of its importance in both lateral stability and maneuverability. Some of the principal points regarding this derivative are illustrated in figure 11 which is a plot of the experimentally determined variation of  $C_{l_p}$  with lift coefficient for swept and unswept wings. The symbols at zero lift coefficient indicate the theoretical values of  $C_{l_p}$  for the swept and unswept wings. Theory indicates no variation in  $C_{l_p}$  with lift coefficient.

The curve shown on figure 11 for the unswept wing is for a wing of aspect ratio 5.2 but it shows characteristics that are typical of unswept wings of all aspect ratios. The experimental value of  $C_{l_p}$  is in agreement with the theory and remains essentially constant from zero lift to the stall but at the stall it abruptly decreases to zero and to positive values which indicates that the wing is unstable in roll beyond the stall and will autorotate or continue to roll once it has started. Various stall-control devices such as leading-edge slots have been used to eliminate the autorotation tendency of unswept wings at the stall because in some cases this tendency causes airplanes to become uncontrollable and to go into spins. Increasing the aspect ratio of unswept wings increases the damping in roll but does not materially alter the characteristics at the stall.

The data of figure 11 show that changing from an unswept to a swept wing causes a pronounced change in the damping-in-roll characteristics. The solid-line curve is for a  $45^\circ$  sweptforward wing and the dashed-line curve for a  $45^\circ$  sweptback wing. Both wings have an aspect ratio of 2.6.

The fact that the swept wings have a smaller value of  $C_{l_p}$  than the unswept wing at zero lift is partly because of the sweepback but mostly because the swept wings are of much lower aspect ratio. (See reference 6.) The experimental data are in agreement with the theory at zero lift. The derivative  $C_{l_p}$  for the sweptforward wing increases rapidly with lift coefficient, however, and at the stall it decreases sharply and becomes positive or unstable as in the case of the unswept wing. The rapid increase of  $C_{l_p}$  with lift coefficient is not accounted for by present theories but it can be explained by the change in span load distribution which takes place on the sweptforward wing.

In the case of the sweptback wing, a slight increase occurs in  $C_{l_p}$  with increasing lift coefficient up to some moderately high lift coefficient and then the  $C_{l_p}$  changes abruptly. This change, however, is more gradual than in the case of the unswept or sweptforward wings and the value of  $C_{l_p}$  remains negative or stable even beyond the stall. For swept wings having a very large amount of sweep or a very small aspect ratio,  $C_{l_p}$  does become unstable at the stall or at even lower lift coefficients. The fact that the sweptback wings of moderate sweep and aspect ratio maintain damping in roll at the stall is very important for it means that any roll-offs at the stall should be less violent than on most unswept wings.

#### EFFECT OF IMPORTANT STABILITY DERIVATIVES ON FLYING CHARACTERISTICS

The effects of the two most important stability derivatives - the directional or weathercock stability derivative  $C_{n\beta}$  and the effective-dihedral derivative  $C_{l\beta}$  - have been the subject of extensive studies, both experimental (references 60 to 68) and theoretical (references 69 to 71). The results of these studies have generally been in good agreement and consequently only a typical set of results will be discussed. The results of an investigation in the Langley free-flight tunnel of the effects of  $C_{n\beta}$  and  $C_{l\beta}$  (reference 65) are presented in figure 12. In this investigation a model was flown with a large number of combinations of vertical-tail area and geometric dihedral which provided the changes in  $C_{n\beta}$  and  $C_{l\beta}$ . The results are plotted in the form of a stability chart with  $C_{n\beta}$  as the ordinate and  $-C_{l\beta}$  as the abscissa and with the flight behavior obtained with the different combinations of  $C_{n\beta}$  and  $C_{l\beta}$  indicated by the crosshatched regions on the chart.

These results are for a lift coefficient of 1.0 and for ailerons-alone control (rudder fixed) and only represent a small part of the results of the comprehensive investigation reported in reference 65.

The stability chart of figure 12 can be explained more clearly by considering the flight behavior of the model with the three combinations of  $C_{n\beta}$  and  $C_{l\beta}$  marked (1), (2), and (3), each within a different region on the chart. Point (1) represents a satisfactory combination because with this condition the model was easy to fly and responded satisfactorily to the controls with little adverse yawing. Point (2), which has a lower value of  $C_{n\beta}$  but the same value of  $-C_{l\beta}$ , was not considered entirely satisfactory because with the decreased weathercock stability excessive adverse yawing occurred during aileron rolls. This point was considered satisfactory when rudder was coordinated with the ailerons to eliminate this adverse yawing. Point (3), which has low  $C_{n\beta}$  and high  $-C_{l\beta}$ , represents an unflyable condition with ailerons alone. In this case, the low weathercock stability permitted excessive adverse yawing which, in combination with the large value of effective dihedral or rolling moment due to sideslip, caused reversal of aileron effectiveness. That is, when right aileron control was given, the model started to roll to the right but it also started to yaw to the left (or sideslip to the right) and the large value of rolling moment due to sideslip  $C_{l\beta}$  then caused large adverse rolling moments which overpowered the ailerons and caused the model to roll to the left instead of to the right. Here again, when the rudder was coordinated with the ailerons, flights could be made but even in this case the flying characteristics were not considered satisfactory because of a weak weathercocking tendency and a lightly damped Dutch roll oscillation. This oscillation is discussed in detail in the next paper "Dynamic Stability," by Sternfield.

#### CONCLUDING REMARKS

During the war years and since the war, a great amount of experimental and theoretical research in the field of lateral stability was carried out and many advances were made toward a better understanding of the problems involved. Much of the information, however, is still not in a form to be used directly in airplane design, and in many cases, further correlation and analysis are required to realize the full potential usefulness of the results.

Some experimental work has been done to determine the effects of Reynolds number, and theoretical work, to determine the effects of Mach number (references 72 to 75) on the various stability derivatives. Much more research appears to be necessary, however, to determine fully these effects. Further studies should also be made of the effects on lateral stability and control of other factors such as aeroelasticity, wing airfoil section and surface roughness, and wing-fuselage-tail interference.

## REFERENCES

1. Zimmerman, Charles H.: An Analysis of Lateral Stability in Power-Off Flight with Charts for Use in Design. NACA Rep. No. 589, 1937.
2. Pearson, Henry A., and Jones, Robert T.: Theoretical Stability and Control Characteristics of Wings with Various Amounts of Taper and Twist. NACA Rep. No. 635, 1938.
3. Jones, Robert T.: Notes on the Stability and Control of Tailless Airplanes. NACA TN No. 837, 1941.
4. Langley Stability Research Division (Compiled by Charles J. Donlan): An Interim Report on the Stability and Control of Tailless Airplanes. NACA Rep. No. 796, 1944.
5. Soulé, Hartley A.: Influence of Large Amounts of Wing Sweep on Stability and Control Problems of Aircraft. NACA TN No. 1088, 1946.
6. Toll, Thomas A., and Queijo, M. J.: Approximate Relations and Charts for Low-Speed Stability Derivatives of Swept Wings. NACA TN No. 1581, 1948.
7. Multhopp, H.: Aerodynamics of the Fuselage. NACA TM No. 1036, 1942.
8. Bamber, M. J., and House, R. O.: Wind-Tunnel Investigation of Effect of Yaw on Lateral-Stability Characteristics. I - Four N.A.C.A. 23012 Wings of Various Plan Forms with and without Dihedral. NACA TN No. 703, 1939.
9. Bamber, M. J., and House, R. O.: Wind-Tunnel Investigation of Effect of Yaw on Lateral-Stability Characteristics. II - Rectangular N.A.C.A. 23012 Wing with Circular Fuselage and a Fin. NACA TN No. 730, 1939.
10. House, Rufus O., and Wallace, Arthur R.: Wind-Tunnel Investigation of Effect of Interference on Lateral-Stability Characteristics of Four NACA 23012 Wings, an Elliptical and a Circular Fuselage, and Vertical Fins. NACA Rep. No. 705, 1941.
11. Recant, Isidore G., and Wallace, Arthur R.: Wind-Tunnel Investigation of Effect of Yaw on Lateral-Stability Characteristics. III - Symmetrically Tapered Wing at Various Positions on Circular Fuselage with and without a Vertical Tail. NACA TN No. 825, 1941.

12. Recant, I. G., and Wallace, Arthur R.: Wind-Tunnel Investigation of Effects of Yaw on Lateral-Stability Characteristics. IV - Symmetrically Tapered Wing with a Circular Fuselage Having a Wedge-Shaped Rear and a Vertical Tail. NACA ARR, March 1942.
13. Wallace, Arthur R., and Turner, Thomas R.: Wind-Tunnel Investigation of Effect of Yaw on Lateral-Stability Characteristics. V - Symmetrically Tapered Wing with a Circular Fuselage Having a Horizontal and a Vertical Tail. NACA ARR No. 3F23, 1943.
14. Teplitz, Jerome: Effects of Small Angles of Sweep and Moderate Amounts of Dihedral on Stalling and Lateral Characteristics of a Wing-Fuselage Combination Equipped with Partial- and Full-Span Double Slotted Flaps. NACA Rep. No. 800, 1944.
15. Purser, Paul E., and Campbell, John P.: Experimental Verification of a Simplified Vee-Tail Theory and Analysis of Available Data on Complete Models with Vee Tails. NACA Rep. No. 823, 1945.
16. Hollingworth, Thomas A.: Investigation of Effect of Sideslip on Lateral Stability Characteristics. II - Rectangular Midwing on Circular Fuselage with Variations in Vertical-Tail Area and Fuselage Length with and without Horizontal Tail Surface. NACA ARR No. L5C13, 1945.
17. Hollingworth, Thomas A.: Investigation of Effect of Sideslip on Lateral Stability Characteristics. III - Rectangular Low Wing on Circular Fuselage with Variations in Vertical-Tail Area and Fuselage Length with and without Horizontal Tail Surface. NACA ARR No. L5C13a, 1945.
18. Lange, Roy H.: Langley Full-Scale-Tunnel Investigation of the Factors Affecting the Static Lateral-Stability Characteristics of a Typical Fighter-Type Airplane. NACA RM No. L6L18, 1946.
19. Letko, William, and Goodman, Alex: Preliminary Wind-Tunnel Investigation at Low Speed of Stability and Control Characteristics of Swept-Back Wings. NACA TN No. 1046, 1946.
20. Imlay, Frederick H.: The Estimation of the Rate of Change of Yawing Moment with Sideslip. NACA TN No. 636, 1938.
21. Pass, H. R.: Analysis of Wind-Tunnel Data on Directional Stability and Control. NACA TN No. 775, 1940.
22. Shortal, Joseph A., and Draper, John W.: Free-Flight-Tunnel Investigation of the Effect of the Fuselage Length and the Aspect Ratio and Size of the Vertical Tail on Lateral Stability and Control. NACA ARR No. 3D17, 1943.



23. Fehlner, Leo F., and MacLachlan, Robert: Investigation of Effect of Sideslip on Lateral Stability Characteristics. I - Circular Fuselage with Variations in Vertical-Tail Area and Tail Length with and without Horizontal Tail Surface. NACA ARR No. L4E25, 1944.
24. Bishop, Robert C., and Lomax, Harvard: A Simplified Method for Determining from Flight Data the Rate of Change of Yawing-Moment Coefficient with Sideslip. NACA TN No. 1076, 1946.
25. Hoggard, H. Page, Jr.: Wind-Tunnel Investigation of Fuselage Stability in Yaw with Various Arrangements of Fins. NACA TN No. 785, 1940.
26. Donlan, C. J., and Letko, W.: The Effect of Cowling Shape on the Stability Characteristics of an Airplane. NACA ARR, Sept. 1942.
27. MacLachlan, Robert, and Levitt, Joseph: Wind-Tunnel Investigation of Effect of Canopies on Directional Stability Characteristics of a Single-Engine Airplane Model. NACA TN No. 1052, 1946.
28. Thompson, F. L., and Gilruth, R. R.: Notes on the Stalling of Vertical Tail Surfaces and on Fin Design. NACA TN No. 778, 1940.
29. Katzoff, S., and Mutterperl, William: The End-Plate Effect of a Horizontal-Tail Surface on a Vertical-Tail Surface. NACA TN No. 797, 1941.
30. Recant, Isidore G., and Wallace, Arthur R.: Wind-Tunnel Investigation of the Effect of Vertical Position of the Wing on a Side Flow in the Region of the Vertical Tail. NACA TN No. 804, 1941.
31. Murray, Harry E.: Wind-Tunnel Investigation of End-Plate Effects of Horizontal Tails on a Vertical Tail Compared with Available Theory. NACA TN No. 1050, 1946.
32. Neely, R. H., Fogarty, L. E., and Alexander, S. R.: Comparison of Yaw Characteristics of a Single-Engine Airplane Model with Single-Rotating and Dual-Rotating Propellers. NACA ACR No. L4D19, 1944.
33. Pitkin, Marvin, Draper, John W., and Bennett, Charles V.: The Influence of Vertical-Tail Design and Direction of Propeller Rotation on Trim Characteristics of a Twin-Engine-Airplane Model with One Engine Inoperative. NACA ARR No. L5A13, 1945.

34. Stevens, Victor I., McCullough, George B., and Hanson, Frederick H.: An Experimental Investigation of the Effect of Propellers Used as Aerodynamic Brakes on Stability and Control. NACA ARR No. 5C01, 1945.
35. Shortal, Joseph A.: Effect of Tip Shape and Dihedral on Lateral-Stability Characteristics. NACA Rep. No. 548, 1935.
36. Maggin, Bernard, and Shanks, Robert E.: The Effect of Geometric Dihedral on the Aerodynamic Characteristics of a  $40^\circ$  Swept-Back Wing of Aspect Ratio 3. NACA TN No. 1169, 1946.
37. Pitkin, Marvin, and Schade, Robert O.: Tests of a Linked Differential Flap System Designed to Minimize the Reduction in Effective Dihedral Caused by Power. NACA ARR No. L5F25, 1945.
38. Drake, Hubert M.: The Effect of Lateral Area on the Lateral Stability and Control Characteristics of an Airplane as Determined by Tests of a Model in the Langley Free-Flight Tunnel. NACA ARR No. L5L05, 1946.
39. Swanson, Robert S., and Priddy, E. LaVerne: Lifting-Surface-Theory Values of the Damping in Roll and of the Parameter Used in Estimating Aileron Stick Forces. NACA ARR No. L5F23, 1945.
40. Bennett, Charles V., and Johnson, Joseph L.: Experimental Determination of the Damping in Roll and Aileron Rolling Effectiveness of Three Wings Having  $2^\circ$ ,  $42^\circ$ , and  $62^\circ$  Sweepback. NACA TN No. 1278, 1947.
41. MacLachlan, Robert, and Letko, William: Correlation of Two Experimental Methods of Determining the Rolling Characteristics of Unswept Wings. NACA TN No. 1309, 1947.
42. Harmon, Sidney M.: Determination of the Damping Moment in Yawing for Tapered Wings with Partial-Span Flaps. NACA ARR No. 3H25, 1943.
43. Cotter, William E., Jr.: Summary and Analysis of Data on Damping in Yaw and Pitch for a Number of Airplane Models. NACA TN No. 1080, 1946.
44. Campbell, John P., and Mathews, Ward O.: Experimental Determination of the Yawing Moment Due to Yawing Contributed by the Wing, Fuselage, and Vertical Tail of a Midwing Airplane Model. NACA ARR No. 3F28, 1943.
45. Stüper, J.: Effect of Propeller Slipstream on Wing and Tail. NACA TM No. 874, 1938.

46. Rogallo, Francis M., and Swanson, Robert S.: Wind-Tunnel Tests of a Twin-Engine Model to Determine the Effect of Direction of Propeller Rotation on the Static-Stability Characteristics. NACA ARR, Jan. 1943.
47. Harper, Charles W., and Wick, Bradford H.: A Comparison of the Effects of Four-Blade Dual- and Single-Rotation Propellers on the Stability and Control Characteristics of a High-Powered Single-Engine Airplane. NACA ARR No. 4F17, 1944.
48. Tamburello, Vito, and Weil, Joseph: Wind-Tunnel Investigation of the Effect of Power and Flaps on the Static Lateral Characteristics of a Single-Engine Low-Wing Airplane Model. NACA TN No. 1327, 1947.
49. Hagerman, John R.: Wind-Tunnel Investigation of the Effect of Power and Flaps on the Static Lateral Stability and Control Characteristics of a Single-Engine High-Wing Airplane Model. NACA TN No. 1379, 1947.
50. Ribner, Herbert S.: Field of Flow about a Jet and Effect of Jets on Stability of Jet-Propelled Airplanes. NACA ACR No. L6C13, 1946.
51. Purser, Paul E., and Spear, Margaret F.: Tests to Determine Effects of Slipstream Rotation on the Lateral Stability Characteristics of a Single-Engine Low-Wing Airplane Model. NACA TN No. 1146, 1946.
52. Ribner, Herbert S.: Notes on the Propeller and Slipstream in Relation to Stability. NACA ARR No. L4I12a, 1944.
53. Ribner, Herbert S., and MacLachlan, Robert: Effect of Slipstream Rotation in Producing Asymmetric Forces on a Fuselage. NACA TN No. 1210, 1947.
54. Phillips, W. H., Crane, H. L., and Hunter, P. A.: Effect of Lateral Shift of Center of Gravity on Rudder Deflection Required for Trim. NACA RB No. L4I06, 1944.
55. Wallace, Arthur R., and Comenzo, Raymond J.: Effect of Engine Skew on Directional and Lateral Control Characteristics of Single-Engine Airplanes. NACA RM No. L6I16, 1947.
56. Zimmerman, C. H.: Characteristics of Clark Y Airfoils of Small Aspect Ratios. NACA Rep. No. 431, 1932.
57. Tosti, Louis P.: Low-Speed Static Stability and Damping-in-Roll Characteristics of Some Swept and Unswept Low-Aspect-Ratio Wings. NACA TN No. 1468, 1947.

58. Murray, Harry E., and Wells, Evalyn G.: Wind-Tunnel Investigation of the Effect of Wing-Tip Fuel Tanks on Characteristics of Unswept Wings in Steady Roll. NACA TN No. 1317, 1947.
59. Maggin, Bernard, and Bennett, Charles V.: Low-Speed Stability and Damping-in-Roll Characteristics of Some Highly Swept Wings. NACA TN No. 1286, 1947.
60. Weick, Fred E., Soulé, Hartley A., and Gough, Melvin N.: A Flight Investigation of the Lateral Control Characteristics of Short Wide Ailerons and Various Spoilers with Different Amounts of Wing Dihedral. NACA Rep. No. 494, 1934.
61. Campbell, John P., and Seacord, Charles L., Jr.: The Effect of Mass Distribution on the Lateral Stability and Control Characteristics of an Airplane as Determined by Tests of a Model in the Free-Flight Tunnel. NACA Rep. No. 769, 1943.
62. McKinney, Marion O., Jr.: Experimental Determination of the Effect of Negative Dihedral on Lateral Stability and Control Characteristics at High Lift Coefficients. NACA ARR No. L5J02, 1946.
63. Drake, Hubert M.: Experimental Determination of the Effects of Directional Stability and Rotary Damping in Yaw on Lateral Stability and Control Characteristics. NACA TN No. 1104, 1946.
64. Ankenbruck, Herman O.: Effects of Tip Dihedral on Lateral Stability and Control Characteristics as Determined by Tests of a Dynamic Model in the Langley Free-Flight Tunnel. NACA TN No. 1059, 1946.
65. McKinney, Marion O., Jr.: Experimental Determination of the Effects of Dihedral, Vertical-Tail Area, and Lift Coefficient on Lateral Stability and Control Characteristics. NACA TN No. 1094, 1946.
66. Maggin, Bernard, and Bennett, Charles V.: Flight Tests of an Airplane Model with a  $42^\circ$  Swept-Back Wing in the Langley Free-Flight Tunnel. NACA TN No. 1287, 1947.
67. Maggin, Bernard, and Bennett, Charles V.: Flight Tests of an Airplane Model with a  $62^\circ$  Swept-Back Wing in the Langley Free-Flight Tunnel. NACA TN No. 1288, 1947.
68. Forsyth, Charles M., and Gray, William E., Jr.: A Comparison of Flight-Test Results on a Scout-Bomber Airplane with  $4.7^\circ$  and with  $10^\circ$  Geometric Dihedral in the Wing Outer Panels. NACA TN No. 1407, 1947.

69. Jones, Robert T.: The Influence of Lateral Stability on Disturbed Motions of an Airplane with Special Reference to the Motions Produced by Gusts. NACA Rep. No. 638, 1938.
70. Fehlner, Leo F.: A Study of the Effects of Vertical Tail Area and Dihedral on the Lateral Maneuverability of an Airplane. NACA ARR, Oct. 1941.
71. Fehlner, Leo F.: A Study of the Effect of Adverse Yawing Moment on Lateral Maneuverability at a High Lift Coefficient. NACA ARR, Sept. 1942.
72. Ribner, Herbert S.: The Stability Derivatives of Low-Aspect-Ratio Triangular Wings at Subsonic and Supersonic Speeds. NACA TN No. 1423, 1947.
73. Jones, Arthur L., and Alksne, Alberta: The Damping Due to Roll of Triangular, Trapezoidal, and Related Plan Forms in Supersonic Flow. NACA TN No. 1548, 1948.
74. Brown, Clinton E., and Adams, Mac C.: Damping in Pitch and Roll of Triangular Wings at Supersonic Speeds. NACA TN No. 1566, 1948.
75. Ribner, Herbert S., and Malvestuto, Frank S., Jr.: Stability Derivatives of Triangular Wings at Supersonic Speeds. NACA TN No. 1572, 1948.

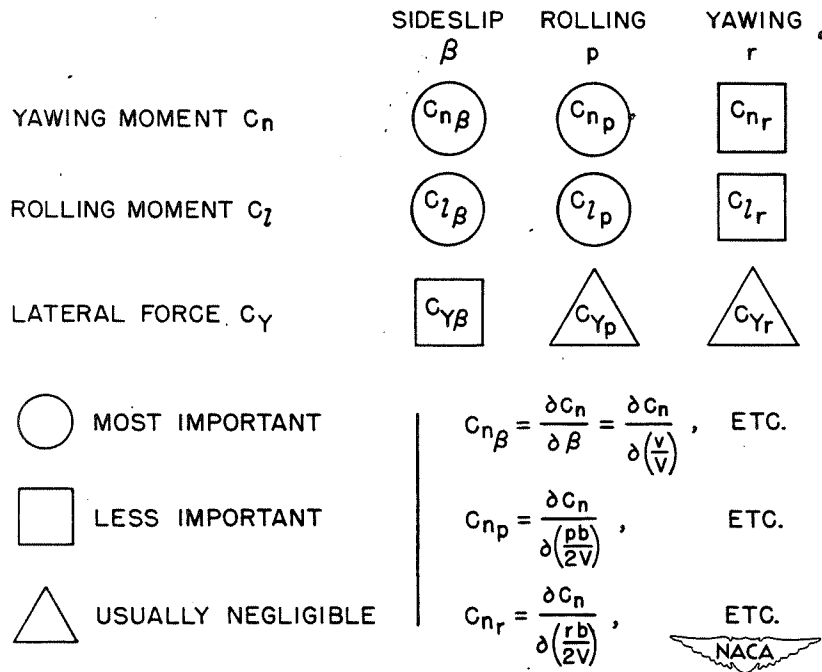


Figure 1.- Lateral-stability derivatives.

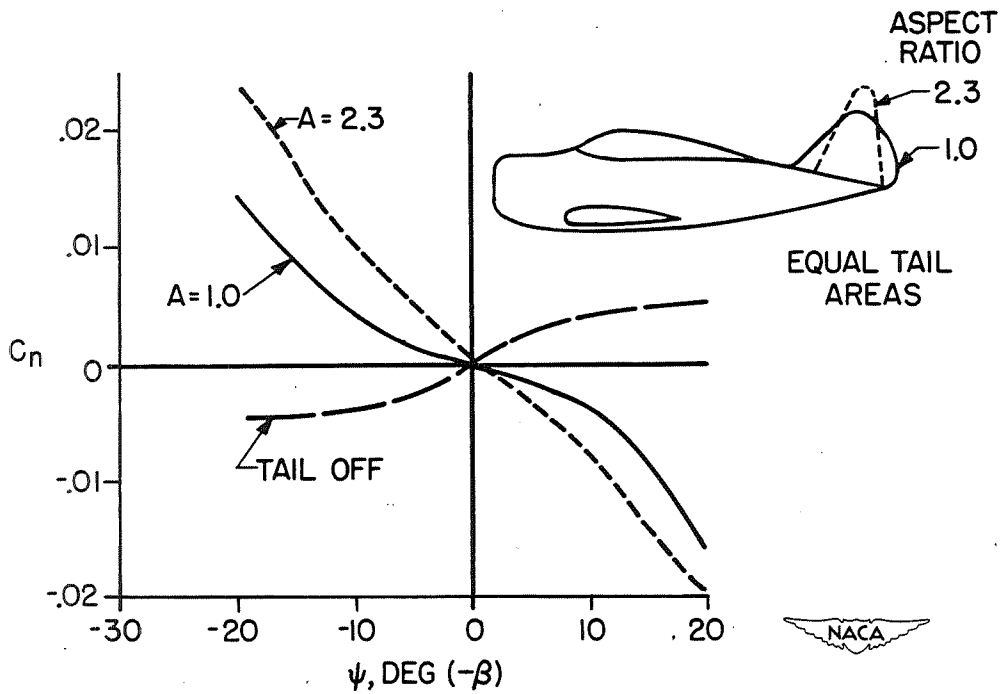


Figure 2.- Effect of aspect ratio of vertical tail on  $C_{n\beta}$ .

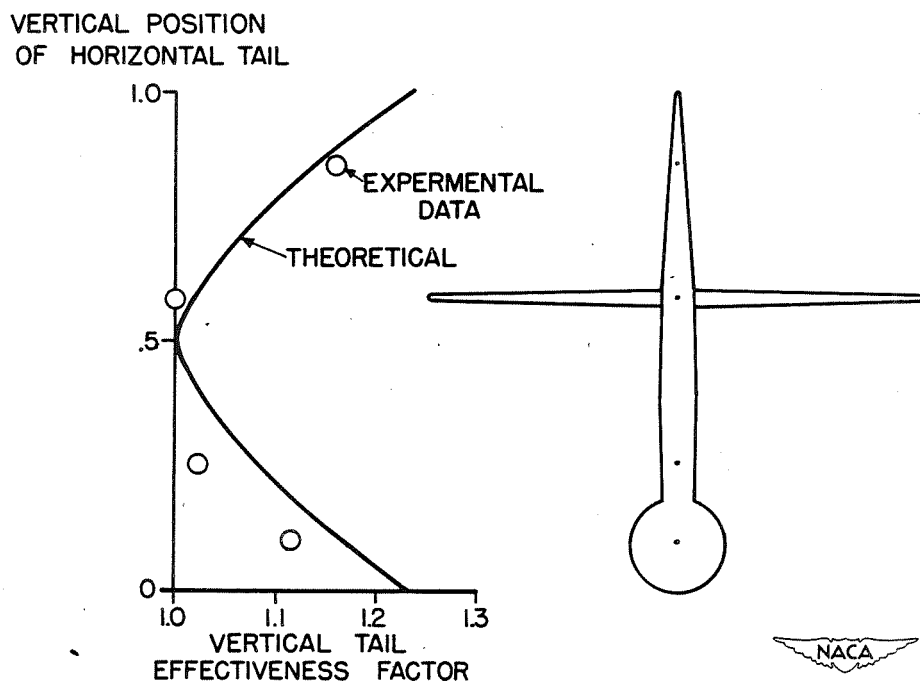


Figure 3.- End-plate effect of horizontal tail on vertical tail.

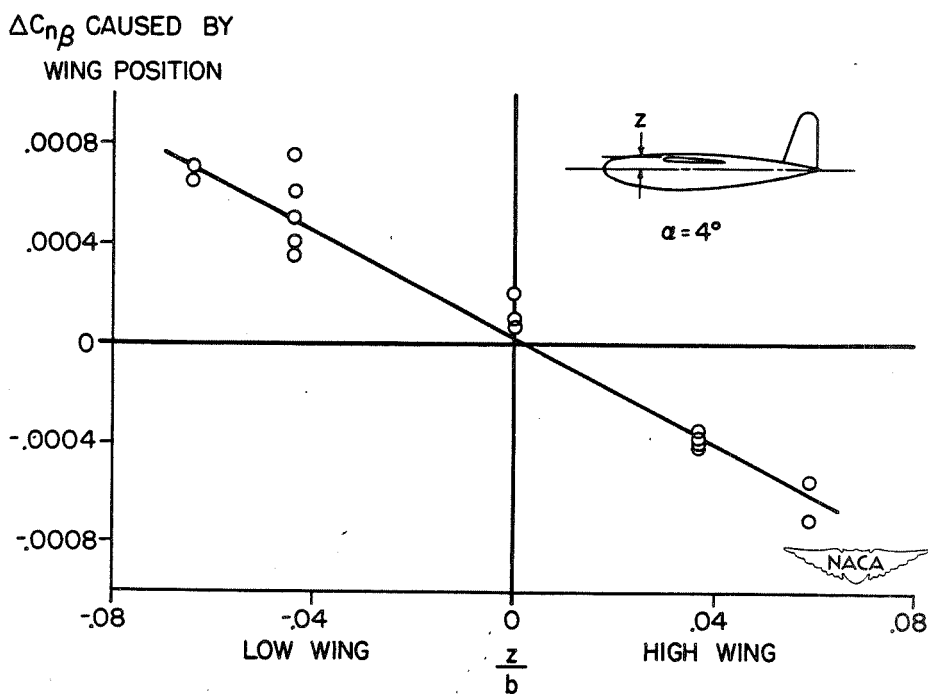


Figure 4.- Effect of wing position on  $C_{n\beta}$ .

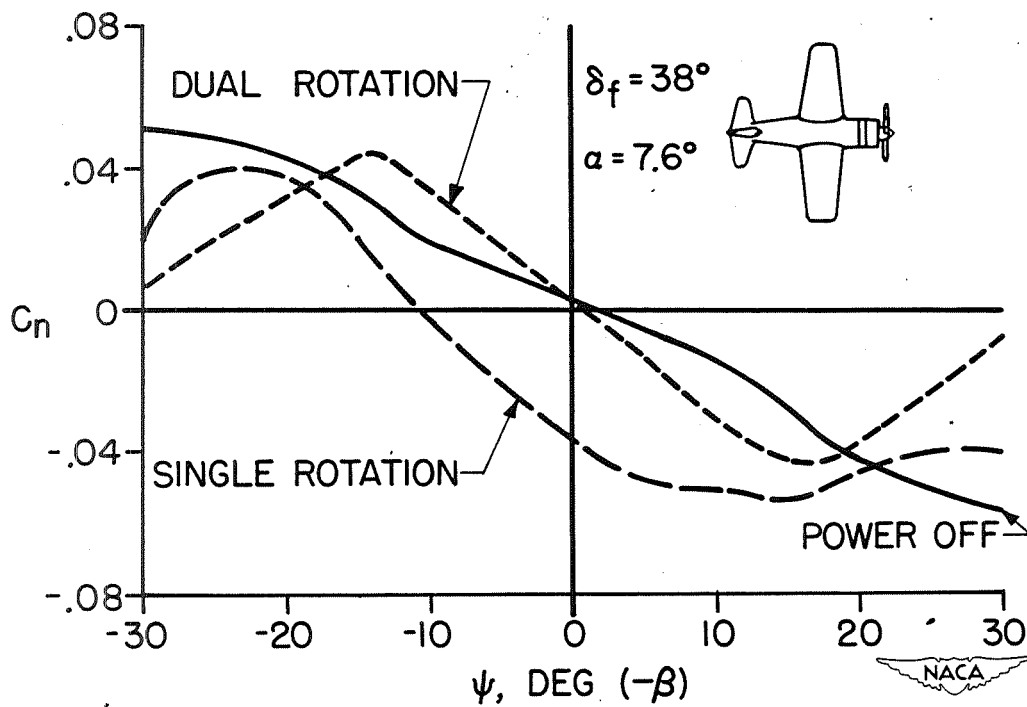


Figure 5.- Effect of power on  $C_{n\beta}$  for a single-engine, propeller-driven airplane.

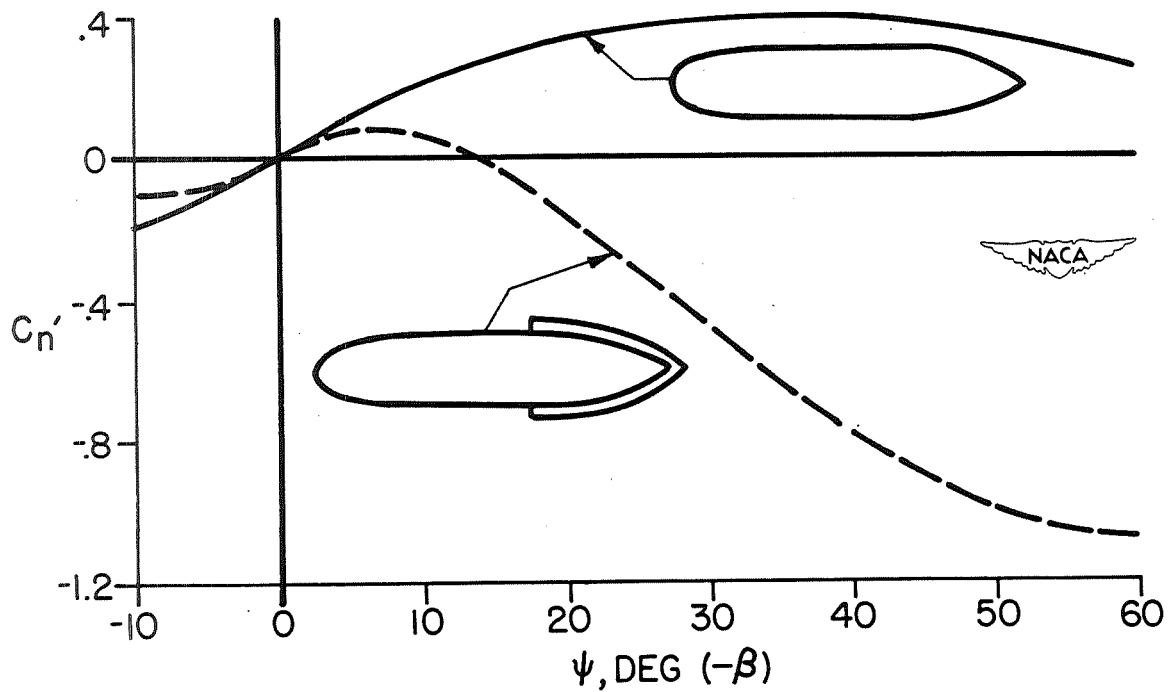


Figure 6.- Effect of dorsal and ventral fins on fuselage instability.



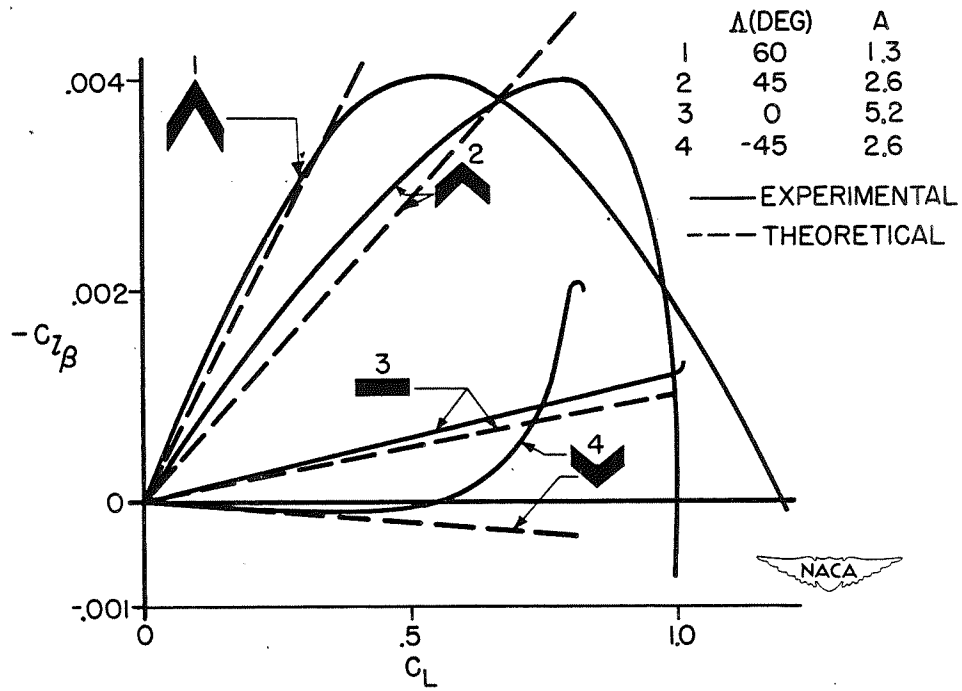


Figure 7.- Effect of wing plan form on  $C_{l\beta}$ .

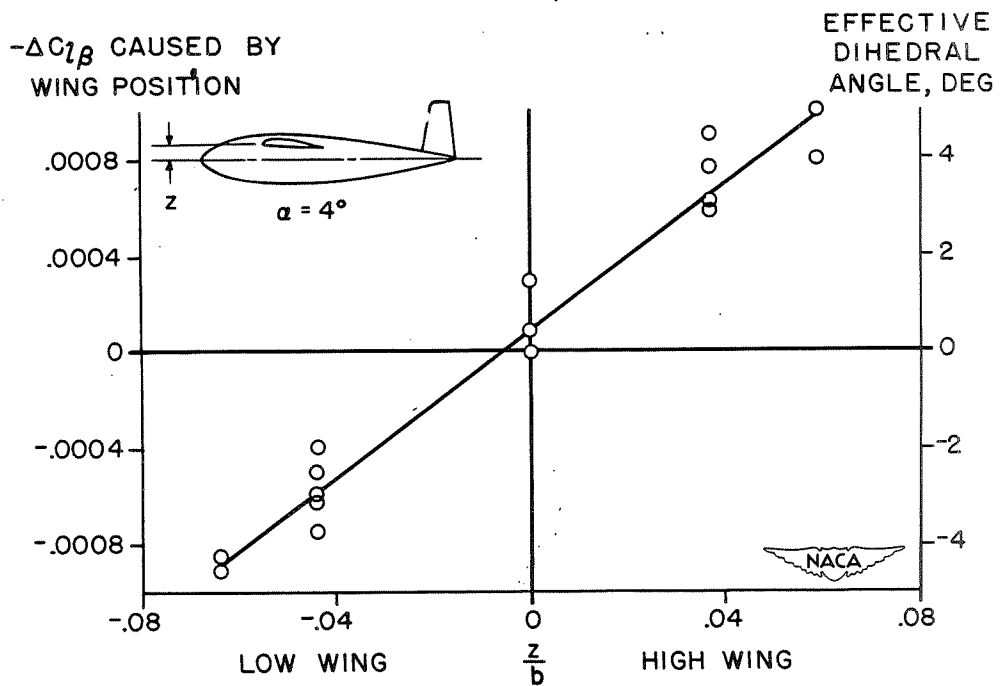


Figure 8.- Effect of wing position on  $C_{l\beta}$ .

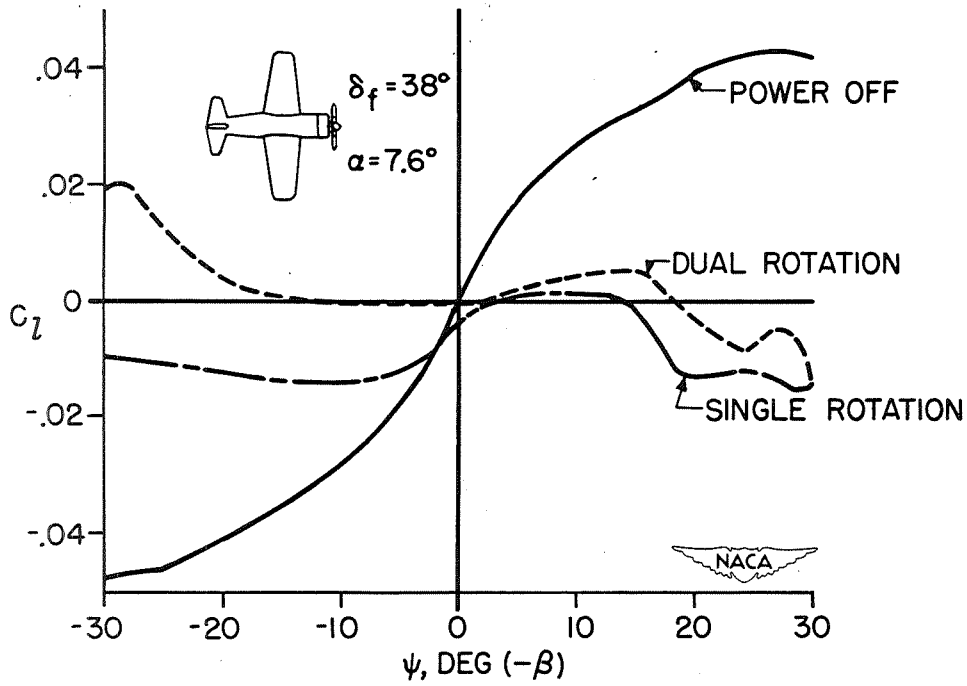


Figure 9.- Effect of power on  $C_{l\beta}$  for a single-engine, propeller-driven airplane.

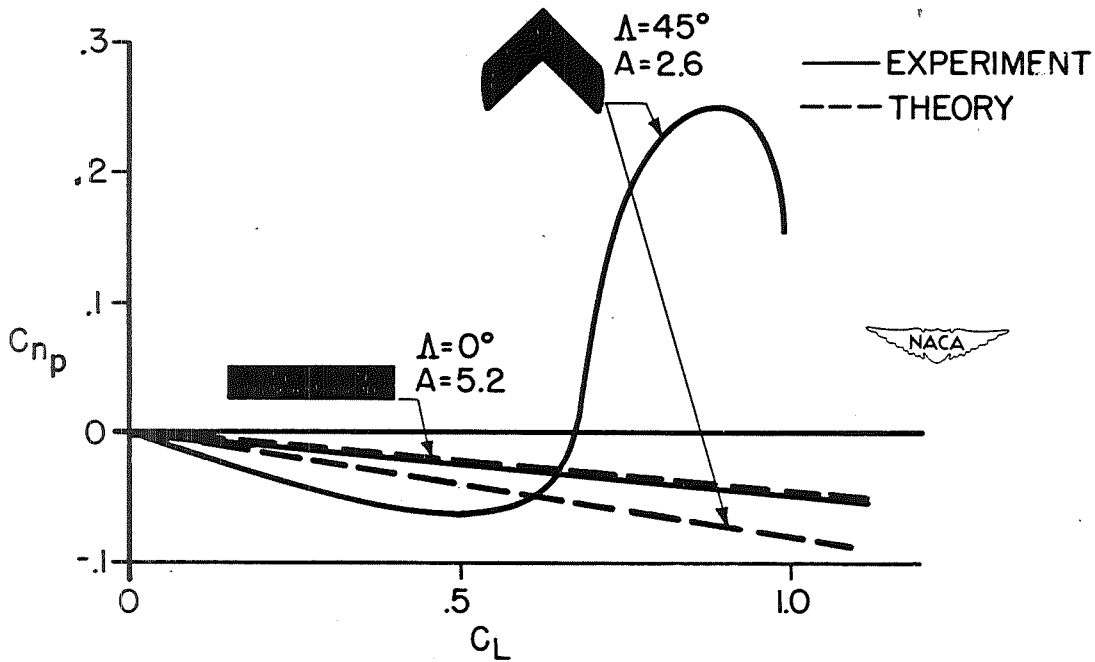


Figure 10.- Effect of wing plan form on  $C_{np}$ .

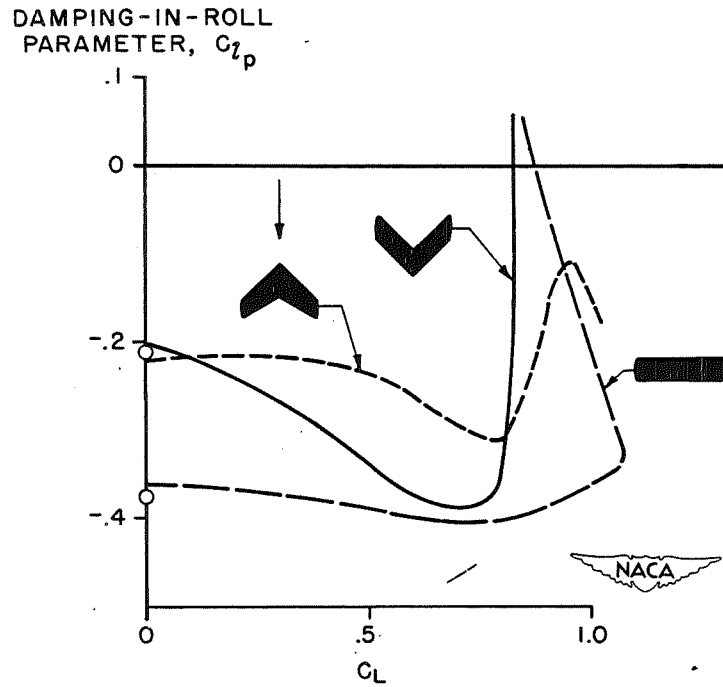


Figure 11.- Effect of wing plan form on  $C_{l_p}$ .

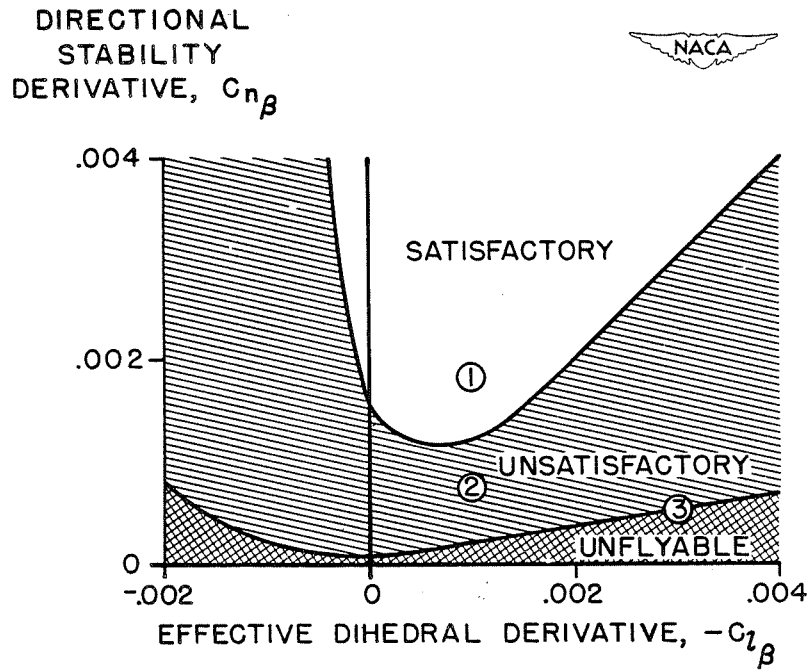


Figure 12.- Flight behavior chart based on model tests in Langley free-flight tunnel. Ailerons alone;  $C_L = 1.0$ .